

Final report

Homo- and heteroepitaxy of transparent semiconducting oxide layers of the Ga_2O_3 - In_2O_3 - Al_2O_3 ternary system on $\beta\text{-Ga}_2\text{O}_3$ and In_2O_3 substrates

Leibniz-Institute: Institut für Kristallzüchtung
Reference number: SAW-2012-IKZ-2
Project period: 01.March 2012- 28.February 2015
Contact partner: Dr. Günter Wagner

Contents:

1. Introduction
2. Surface preparation of oxide substrates for MOCVD epitaxy of III-group oxides
3. Deposition of β -Ga₂O₃ layers on Al₂O₃ (0001) substrates
4. Homoepitaxial growth of β -Ga₂O₃ layers
 - 4.1 β -Ga₂O₃ deposition by using trimethylgallium (TMGa) and pure oxygen
 - 4.2 β -Ga₂O₃ deposition by using trimethylgallium and water as oxygen source
5. Deposition of (Ga_{1-x}In_x)₂O₃ layers on Al₂O₃ substrates
6. Effect of indium as a surfactant in (Ga_{1-x}In_x)₂O₃ epitaxial growth on Ga₂O₃
7. n-type doping of β -Ga₂O₃ layers
 - 7.1 Ga₂O₃ layers doped by Si using tetraethylorthosilicate (Si(OC₂H₅)₄)
 - 7.2 Ga₂O₃ layers doped by Sn using tetraethyltin (Sn(CH₃)₄)
8. β -Ga₂O₃ deposition by using triethylgallium (TEGa) and pure oxygen
9. Summary
10. Technical applicability of the scientific results
11. Educate and qualification activities
12. Dissemination and storing of the scientific results

1. Introduction

The study and development of transparent metal oxides as a new class of semiconductors is a rapidly expanding research field that could lead up to the realization of innovative devices and the understanding of new exciting physics. β - Ga_2O_3 has been widely studied in the last years, emerging as one of the most interesting example in this class of materials. β - Ga_2O_3 has a large band gap of 4.8 eV and an expected breakdown electric field in the range of 8 MV/cm. These excellent material properties can be the basic for application in deep-UV photodetectors [1, 2] and power-devices [3]. Homoepitaxy of Ga_2O_3 thin films has been performed in the recent years mainly by molecular beam epitaxy (MBE), leading to the fabrication of Schottky barrier diodes and field-effect transistors (MESFETs) [4, 5]. Up to now, the homoepitaxy of Ga_2O_3 by metal organic vapour phase epitaxy (MOVPE), which is more suitable for large scale production and faster commercialization of the prototype devices, has been performed mainly by our group at IKZ.

In 2011 the IKZ has successfully submitted a proposal in the call "Pakt für Forschung" of the Leibniz Gemeinschaft. The topic of the proposal is the deposition and characterization of single crystalline transparent semiconducting oxide layers as a new class of semiconductors.

In March, 2012 the three year project started.

A new team was formed, consisting of two scientists, a PhD student and a technician. A guest scientist joined the group in September 2012. The experimental method for the deposition of the hetero- and homoepitaxial layers is a metal-organic chemical vapor phase deposition (MOCVD) system, which was funded from the budget of the IKZ in 2011. It was delivered in March and finally installed in April 2012. Parallel to the preparation of the laboratory and the installation of the MOCVD-system investigations were started to make the oxide substrates epi-ready.

The work plan 2012 included the deposition of Ga_2O_3 layers on Al_2O_3 and Ga_2O_3 substrates to find a set of growth parameters to grow the β - Ga_2O_3 phase modification. In the starting phase of the project, the layer depositions were performed on sapphire substrates because the Ga_2O_3 substrates are rare and not commercially available. Moreover, some additional investigations to study the replacement of gallium-atoms by indium-atoms in the β - Ga_2O_3 lattice and the incorporation of silicon as an n-type doping element in β - Ga_2O_3 have been carried out.

In the second of the three years of the project, the activities were concentrated on three topics:

- Homoepitaxial growth of β - Ga_2O_3 films
- Substitution of Ga atoms by In atoms in the β - Ga_2O_3 lattice
- Incorporation of Sn to tune the electrical properties of the grown layers

In the third year of the project, the research activities were focused on two main topics:

- The improvement of the structural perfection of Ga_2O_3 layers by using indium as surfactant during the layer growth.
- The development of n-type conductive Ga_2O_3 layers.

In this project all research activities were concentrated on growing of Ga_2O_3 and $(\text{Ga}_{1-x}\text{In}_x)_2\text{O}_3$ layers on Al_2O_3 and Ga_2O_3 substrates and on tuning their electrically properties. During the preparation of the proposal, it was not possible to estimate the complexity of the individual topics. The extension of the research on In_2O_3 substrates and the substitution of Ga by Al in Ga_2O_3 to grow $(\text{Ga}_{1-x}\text{Al}_x)_2\text{O}_3$ ternary layers was not under investigation. This topic is a challenge for further complex research activities.

All these activities were conducted in a strong co-operation with the IKZ-groups of physical, x-ray and transmission electron microscopy characterization.

2. Surface preparation of oxide substrates for MOCVD epitaxy of III-group oxides

For the MOCVD growth experiments we have selected Al_2O_3 (0001), Ga_2O_3 (100), and Si (001) substrates. Our purpose was to prepare the surface of the substrates for MOCVD epitaxial growth experiments, i.e. to get a surface without subsurface damage, and to find out the best conditions for step formation that is advantageous for a step flow growth.

The as-received mirror-like polished Al_2O_3 (0001) and $\beta\text{-Ga}_2\text{O}_3$ (100) wafers of $10 \times 10 \text{ mm}^2$ size were ultrasonically cleaned in acetone and isopropanol and their surface morphology was studied by high-resolution AFM in a non-contact mode.

On the basis of the existing literature [6] we decided the oxide substrates to be subjected to high-temperature annealing in oxygen containing environment. Since the Al_2O_3 (0001) and $\beta\text{-Ga}_2\text{O}_3$ (100) substrates are nominally 0.3° off-oriented with respect to c-axis (specification from CrysTec GmbH), the surface of the substrates should exhibit a terraced structure after thermal treatment. The temperature interval for the treatment was chosen between 900 and 1100°C . Figures 1(a) and (b) show an atomic force microscope (AFM) image and surface roughness (RMS) lines scan of the as-supplied Al_2O_3 (0001) substrate. Its surface has irregular small corrugations ranging from 200 to 800 pm , suggesting the existence of the topmost atomic plane different from the (0001) plane or of a residual damage layer on the atomic scale. The investigated surface area (representative for the whole sample) is rather flat with a roughness (rms) of about 40 pm .

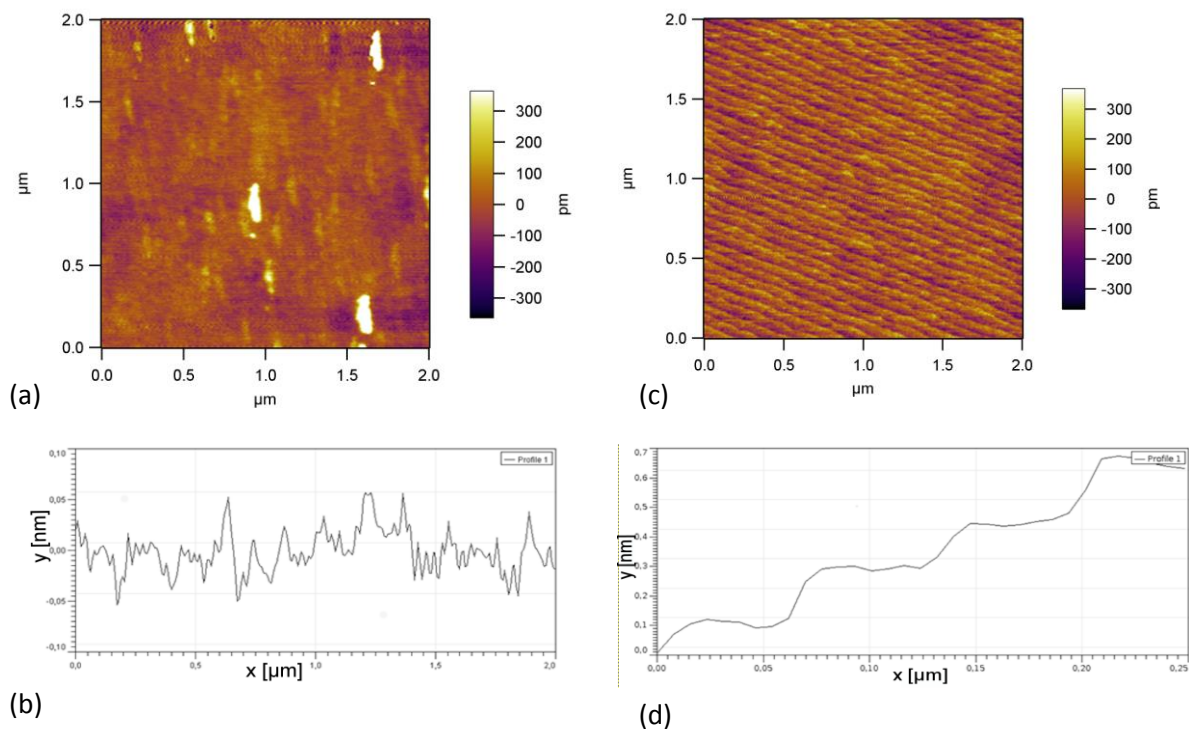


Fig. 1: (a) AFM-image and (b) RMS lines scan of an as-received Al_2O_3 (0001) substrate. (c) AFM image and (d) RMS lines scan of a sapphire (0001) surface after annealing at 950°C , 1 hour in oxygen-containing environment

The AFM image of sapphire substrate surface annealed at a temperature of 950°C for 1 hour in oxygen containing environment is shown in Fig. 1(c). A drastic change in surface morphology was detected, since the irregularly roughened surface in Fig. 1(b) turned into the atomic flat surface with $\sim 0.220 \text{ nm}$ high steps and $\sim 70 \text{ nm}$ wide terraces of Fig. 1(d). The real misorientation angle with respect to (0001) was estimated from the ratio of terrace width to the step height to be about 0.2° .

A similar study has been performed for the Ga_2O_3 (100) substrates. Fig. 2 illustrates a typical AFM image of the surface morphology of Ga_2O_3 (100) substrate annealed at 1000°C for one hour in oxygen-containing atmosphere. The estimated terrace width is 70-100 nm and the step height 0.60 nm respectively.

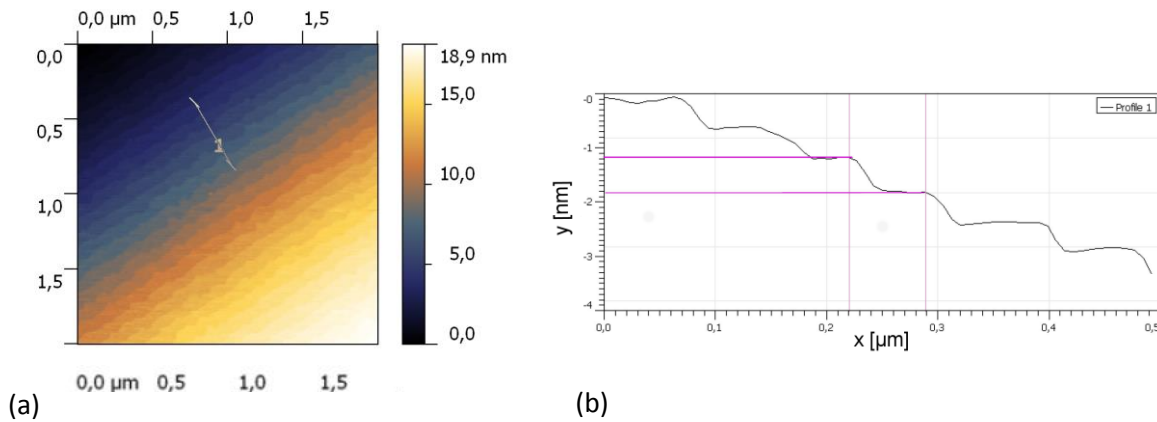


Fig. 2: (a) AFM image and (b) RMS lines scan of a $\beta\text{-Ga}_2\text{O}_3$ (100) surface after 1 hour annealing at 1000°C , in oxygen-containing environment

3. Deposition of $\beta\text{-Ga}_2\text{O}_3$ layers on Al_2O_3 (0001) substrates

The deposition experiments were performed at temperatures between 750 and 850°C . As precursors, we used trimethylgallium (TMGa) and oxygen. Argon was used as carrier gas. Figure 3 shows an AFM image of the surface of a $\beta\text{-Ga}_2\text{O}_3$ layer grown at 800°C on sapphire. The layer grown on Al_2O_3 (0001) at a temperature of 750°C has an amorphous or polycrystalline structure, while at higher temperatures the $\beta\text{-Ga}_2\text{O}_3$ modification is effectively grown. Figure 4 shows the x-ray diffraction (XRD) standard θ - 2θ scan of $\beta\text{-Ga}_2\text{O}_3$ layers grown on Al_2O_3 (0001) at 750 and 800°C .

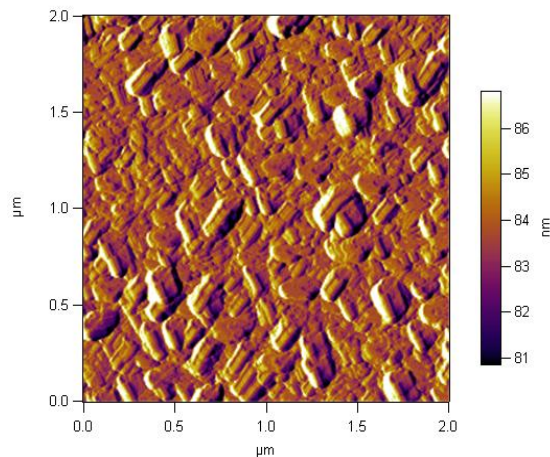


Fig. 3. AFM image of a $\beta\text{-Ga}_2\text{O}_3$ layer surface on Al_2O_3 (0001), thickness: 165 nm, deposition temperature: 800°C

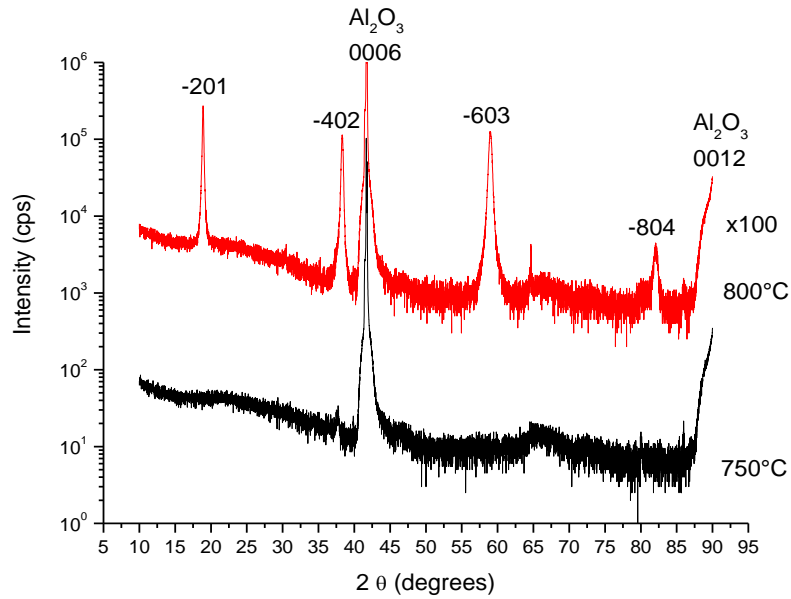


Fig. 4: XRD θ - 2θ -scans of β - Ga_2O_3 layers deposited on Al_2O_3 (0001). The deposition temperatures were 750 and 800°C

All strong diffraction peaks in the curves stem from β - Ga_2O_3 and Al_2O_3 (0001). The peaks at $2\theta = 41.7^\circ$ and 64.5° correspond to the diffractions of the (0006) and (0009) plane of the sapphire substrate. All the identified layer peaks belong to the (-201) plane family of β - Ga_2O_3 . These results indicate that the layer grown at 800°C has the epitaxial relationship (-201) β - Ga_2O_3 II (0001) Al_2O_3 . To get more information about the crystal orientation of these layers, X-ray diffraction pole figures were measured. Figure 5 shows the diffraction intensity distribution from the (-401) plane. The incident and diffraction angles, Θ , were set at $2\Theta=30.46^\circ$. Six strong diffraction peaks are visible. The diffraction peaks, split over 60° of rotation angle, Φ , identify six different types of β - Ga_2O_3 crystals. It is concluded that the β - Ga_2O_3 layer formed on the (0001) plane of sapphire is (-201) oriented and is rotated about the direction normal to the (-201) plane. In Figure 6 are reported the optical transmission spectra in the UV-VIS range for samples grown by TMGa and H_2O . After the subtraction of the substrate contribution, the effective transmittance of the layers is very high ($\sim 90\%$).

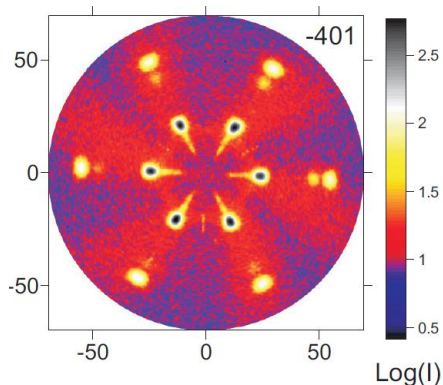


Fig. 5: Pole figure of (-401) plane of β - Ga_2O_3 layer grown on (0001) Al_2O_3

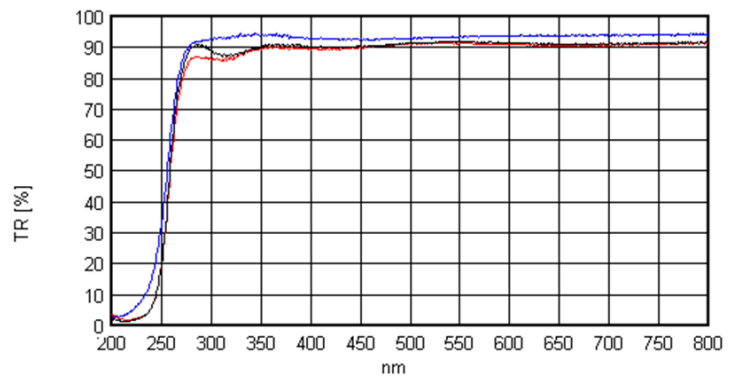


Fig. 6: Typical VIS-UV transmission spectra of β - Ga_2O_3 layers grown on (0001) Al_2O_3 by TMGa and H_2O

Additional characterization by energy dispersive X-ray spectroscopy and electrical measurements has shown that the β - Ga_2O_3 thin films are stoichiometric and insulating.

4. Homoepitaxial growth of β -Ga₂O₃ layers

One side polished 1x1 cm² β -Ga₂O₃ substrates were used, obtained by high quality n-type single crystals grown by the Czochralski method in IKZ. The oxide bulk growth group at the IKZ has long-standing experience and a worldwide reputation for high-temperature melt growth of oxides and fluorides. In particular, during the last five years, IKZ achieved a worldwide leading position in the field of crystal growth of truly bulk semiconducting/conducting oxide crystals, including β -Ga₂O₃, In₂O₃, SnO₂ and MgGa₂O₄ [7-11]. The β -Ga₂O₃ substrates were produced in co-operation with the company CrysTec GmbH, Berlin.

The epitaxial growth of β -Ga₂O₃ was carried out in a commercial vertical MOVPE reactor (SMI inc., USA) at low-pressure conditions [12]. The structural properties of the β -Ga₂O₃ layers were analysed in close co-operation with the IKZ groups Physical Characterization and Electron Microscopy by means of high resolution X-ray diffraction and transmission electron microscopy. In addition, spectroscopic ellipsometry, atomic force microscopy together with scanning electron microscopy investigations were carried out in order to determine the layer thickness and their surface morphology, respectively. Capacitance-voltage and conductivity measurements have been performed to characterize the electrical properties of the grown layers.

4.1 β -Ga₂O₃ deposition by using trimethylgallium (TMGa) and pure oxygen

To prevent dissociation of the Ga₂O₃-substrate surface an oxygen flux of 400 sccm was maintained in the reactor during the heating up to the growth temperature and during cooling down. At first, the Ga₂O₃ homoepitaxy was performed with the same experimental parameters used for the growth on sapphire substrates, but this revealed completely different growth results. The samples were characterized by three-dimensional growth of β -Ga₂O₃ grains up to two-dimensional structures of nanometric size. Figure 7(a) shows a SEM image of a layer surface after growing for 15 min at a temperature of 775°C and chamber pressure of 20 mbar, under Ga and oxygen fluxes of 5 and 400 sccm, respectively.

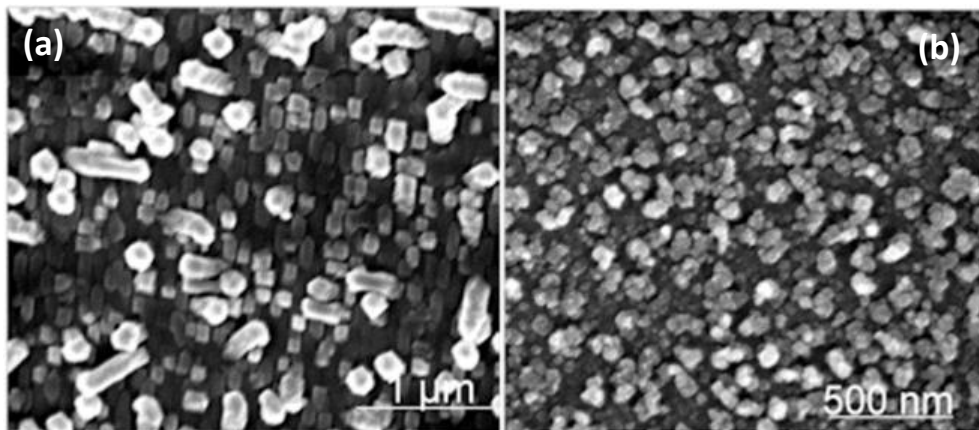


Fig. 7: SEM-images of β -Ga₂O₃ crystals grown on a β -Ga₂O₃ substrate from TMGa and pure oxygen: T_a = 775°C, O/Ga ratio = 1200 (a); T_a = 800°C; O/Ga ratio = 3200 (b)

β -Ga₂O₃ deposited in the form of long wires, up to 500 nm in length and up to 100 nm in diameter, preferentially (100)-oriented. At a deposition temperature of 800°C and increased oxygen-to-gallium ratio of 3200 the grown Ga₂O₃ material looked like an agglomeration of nanocrystals [Fig. 7(b)].

It has to be mentioned, that all wires are growing epitaxially but the coherency of the layer is lost. All attempts to deposit closed homoepitaxial layers of β -Ga₂O₃ on (100) oriented β -Ga₂O₃ substrates using oxygen and TMGa failed, although the growth parameters were varied in a wide range: substrate temperatures between 750 and 850°C, chamber pressure between 5

and 100 mbar, and oxygen-to-gallium ratios up to 9500 were used. In all cases, only β -Ga₂O₃ nano-crystals (either wires or agglomerates) were obtained. This suggests that pure oxygen is not suitable to grow β -Ga₂O₃ homoepitaxial layers with TMGa. For this reason we turned the attention to another source of oxygen, namely water vapour.

4.2 β -Ga₂O₃ deposition by using trimethylgallium and water as oxygen source

Trimethylgallium and ultra pure water were used as precursors and Ar as the carrier gas. The temperature of the water bubbler was fixed at 50°C and the pressure at 300 mbar. The chosen deposition temperature of 800°C represents a compromise between deposition efficiency and crystalline quality. With increasing deposition temperature a decrease of the growth rate was observed. This is due to formation and desorption of gallium suboxide, Ga₂O, which is formed more readily at higher temperatures. On the other hand, for the initial step of nucleation as well as for the subsequent layer growth a higher substrate temperature is desirable since it increases the species mobility on the growth interface and improves the growth kinetics. After a deposition time of 30 minutes a layer of about 170 nm was grown. A typical layer surface morphology as measured by SEM and AFM is shown in Figure 8(a) and (b), respectively. The surface of the grown layer presents a terrace-like morphology similar to the β -Ga₂O₃ substrate but with strong tendency to step bunching.

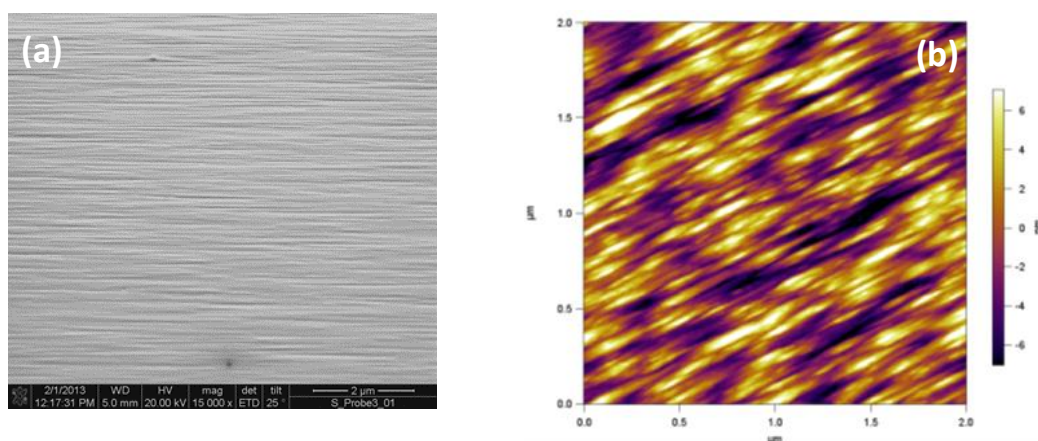


Fig. 8: SEM (a) and AFM (b) images of a β -Ga₂O₃ homoepitaxial layer grown at 800°C and 20 mbar chamber pressure. Layer thickness of about 170 nm, RMS: 6.5 nm

The structural properties of the β -Ga₂O₃ epitaxial layers were characterized by high resolution XRD diffraction pattern and high resolution transmission electron microscopy. As-grown layers showed sharp XRD-peaks that were assigned to the monoclinic gallium oxide phase and odd reflections that could be assigned to plane deformation by extended defects. The high density of stacking faults and twins in the epitaxial β -Ga₂O₃ layer that is found in TEM images (Figure 9) induces strong vertical stacking disorder.

The presence of hydrogen has a positive effect on kinetic conditions of the substrate surface and hence may support the layer-by-layer growth. The influence of the oxygen precursor on the growth mode may be qualitatively discussed as follows. When pure O₂ is employed the formation energy of oxygen vacancies is substantially increased which in turn lowers their concentration. At the same time H₂O and CO₂ are present in comparable concentrations, which can promote the formation of Ga₂(CO₃)₃ at the growth surface as described above. Such compounds act as a mask and whiskers grow out of the unmasked areas. On the other hand when H₂O is employed the oxygen partial pressure is considerably lower and oxygen vacancies are expected to form spontaneously. Since H₂O is present at much higher concentrations than CO₂ the adsorption of CO₂ is prevented and H₂O will spontaneously dissociate at oxygen vacancy sites thus promoting growth. An additional mechanism can also

take place: hydrogen may occupy oxygen vacancy sites by forming Ga-H species and reduce the surface state density. As a consequence, the chemical potential of the surface will be more homogeneous and diffusion of desorbed atoms on the surface will be enhanced. Therefore, the relatively high partial pressure of hydrogen deriving from water dissociation could have a positive effect on the kinetics at the substrate surface and hence support the layer-by-layer growth.

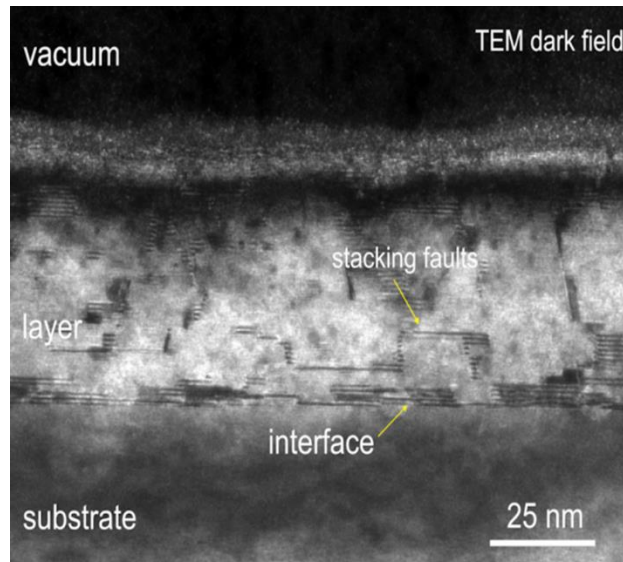


Fig. 9: Dark field TEM image of a β -Ga₂O₃ homoepitaxial layer

5. Deposition of (Ga_{1-x}In_x)₂O₃ layers on Al₂O₃ substrates

Starting from the best growth conditions applied for the Ga₂O₃ deposition, small amounts of trimethylindium (TMIn) were introduced in the reactor additionally to TMGa and O₂ in order to obtain (Ga_{1-x}In_x)₂O₃ as a single phase compound [13]. Al₂O₃ (0001) wafers were used as substrates. The purpose of such experiments is the modulation of the energy gap of the material between the values of Ga₂O₃ (4.8 eV) and In₂O₃ (2.9 eV) [14], and the study of lattice distortion and internal stress effects introduced in the crystal matrix, by substituting Ga³⁺ ($r_{\text{ion}}=0.62 \text{ \AA}$) with a bigger ion as In³⁺ ($r_{\text{ion}}=0.81 \text{ \AA}$).

Different indium atomic fractions in the gas phase, in the range 1-15% with respect to Ga were tested. At first, pure O₂ gas was used as oxygen source. XRD spectra showed a high crystalline degree of the layers, but it also turned out that even at low indium concentration some diffraction peaks relative to In₂O₃ appeared, indicating the presence of a secondary phase. VIS and UV absorption characterization did not show a shift in the optical absorption edge towards lower energies, as expected in case of a pure (Ga_{1-x}In_x)₂O₃ phase.

Different growth temperatures (from 800° to 875°C) and O₂ flows (from 500 to 2500 sccm) were investigated in order to find the best growth conditions, showing that the decrease of both temperature and O₂ flow leads to higher growth rate (essential in view of a technological application) and to better surface morphology, with larger crystalline grains [Fig. 10(a)].

In another series of experiments we used water as an alternative source for oxygen. In this case the surface morphology appeared to be smoother and it was possible to detect a 2D-like growth nucleation [Fig. 10(b)]. However, the layers lost part of their transparency, showing a decrease in the light transmission from 95% (O₂) to 80% (H₂O). This probably indicates that the compound is not perfectly stoichiometric, but has an oxygen deficiency.

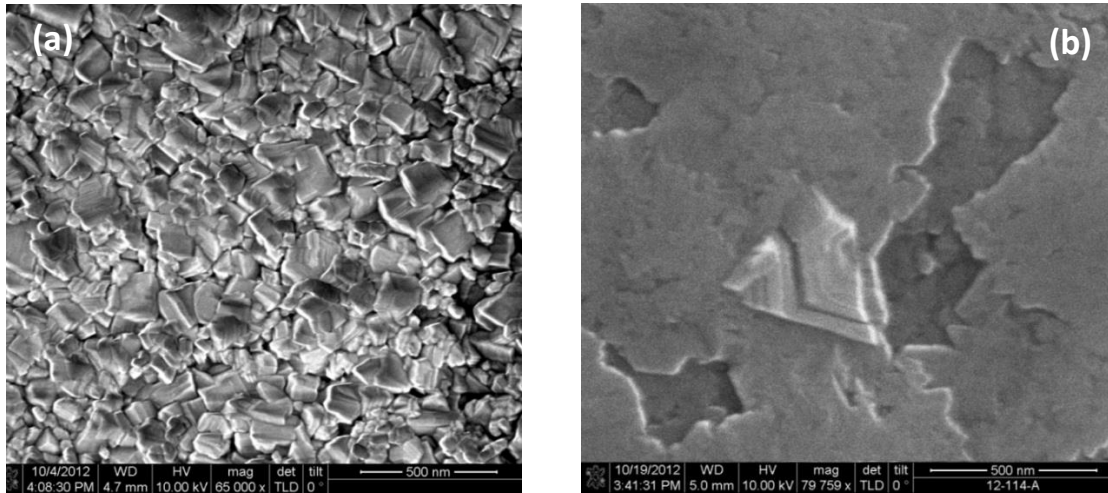


Fig. 10: SEM images of $(\text{Ga}_{1-x}\text{In}_x)_2\text{O}_3$ samples with nominal $x=0.05$ In content, grown at 800°C by using (a) 500 sccm O_2 flow and (b) 200 sccm flow of the alternative O_2 -source

By using the optimal growth parameters identified for pure Ga_2O_3 ($P = 5$ mbar, $T = 800^\circ\text{C}$, $\text{TMGa} = 5$ sccm, $\text{H}_2\text{O} = 200\text{-}500$ sccm), indium was not detectable as a component of the layers by energy-dispersive X-ray (EDX) spectroscopy, even at very high TMIn molar flow rates, up to 1×10^{-5} mol/min (the same of TMGa). The only visible effect of inserting such a high amount of In into the reactor was a drastic decrease of the growth rate. This behavior shows that TMIn reacts directly with H_2O and then the resulting compounds whether desorb too fast from the layers to be correctly incorporated or are directly expelled through the exhaust system. By increasing the TMIn flow, more and more H_2O is consumed by In and Ga has not enough oxygen to react with, forming a thinner and thinner Ga_2O_3 layer. XRD spectra are identical to those of samples grown by O_2 , except for the absence of In_2O_3 -related peaks, confirming the growth of stoichiometric Ga_2O_3 and the epitaxial correlation of the (-201) Ga_2O_3 planes with the (0001) Al_2O_3 ones.

Since in presence of H_2O , indium seems to form very volatile compounds, the reactor base pressure was increased, in order to minimize the desorption process. This expedient revealed to be successful: the amount of In in the layers increases almost linearly with the reactor pressure at constant TMIn flux. Moreover, by fixing the pressure at values comprised between 50 and 200 mbar, the In percentage is proportional to the amount of TMIn introduced into the reactor. On the other side, since the growth rate decreases with increasing both pressure and TMIn flux, a compromise must be achieved in order to grow layers with a definite amount of In in a reasonable lapse of time.

$(\text{Ga}_{1-x}\text{In}_x)_2\text{O}_3$ samples grown at “high” pressure maintain the typical Ga_2O_3 x-ray diffraction (XRD) pattern for a wide In concentration range (Fig. 11). With the above-mentioned experimental conditions, the solubility limit of In in $(\text{Ga}_{1-x}\text{In}_x)_2\text{O}_3$ is $\sim 10\%$ in atomic percent, corresponding to a partial In composition of $x = 0.25$. At higher values phase separation occurs due to the different crystallographic systems of Ga_2O_3 and In_2O_3 , with the diffraction peaks relative to the latter that become sharper and sharper. By observing in detail the 2θ position of XRD peaks, a shift towards smaller angles in respect to the bulk values is clearly visible (inset of Fig. 11). Since the shift increases with In content, this phenomenon can be correlated to the increase of the lattice parameter of Ga_2O_3 due to the substitution of Ga^{3+} with In^{3+} . The mixed $(\text{Ga}_{1-x}\text{In}_x)_2\text{O}_3$ phase is, therefore, effectively achieved.

A confirmation of this result comes from optical absorption measurements. The transparency of the layer, which remains between 80% and 90% from the absorption edge to the long-wavelength region, is a little lower in comparison to samples grown with O_2 , but the most relevant feature of the spectra is the presence of a single absorption edge for samples with In content lower than 10%. In O_2 -based growths, on the contrary, a double step feature always

appeared at about 330 nm, corresponding to the 3.7 eV optical energy gap of In_2O_3 , becoming more and more pronounced as the In content increases.

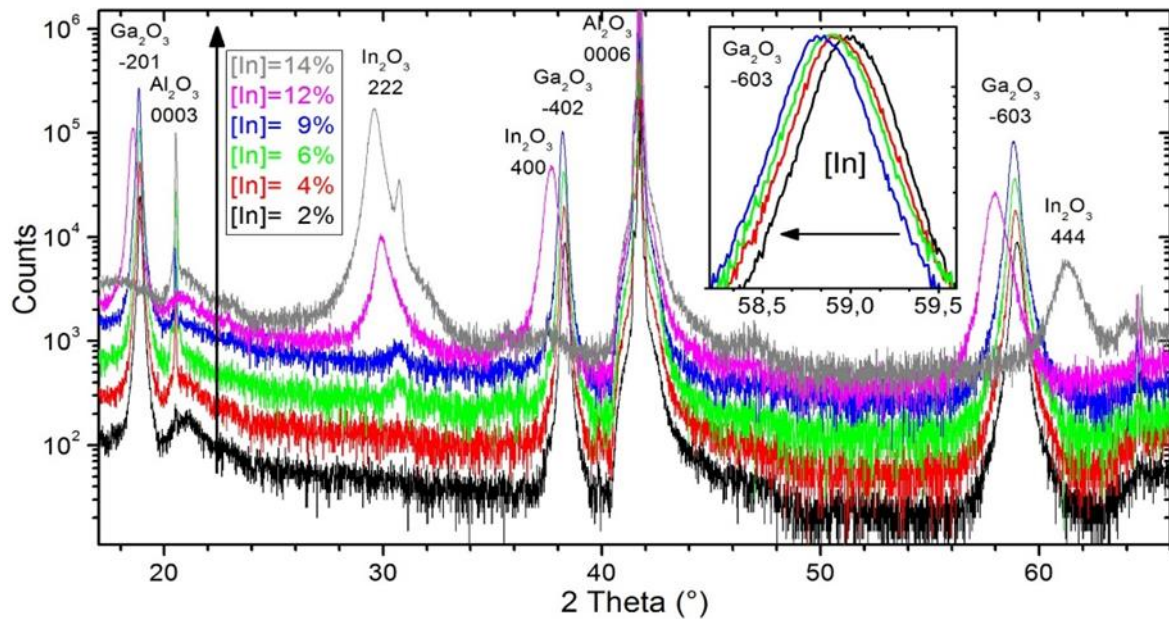


Fig. 11: XRD spectra of $(\text{Ga}_{1-x}\text{In}_x)_2\text{O}_3$ layers on Al_2O_3 grown with increasing In content from 2% (bottom) to 14% (top). Inset: detail of (603) $\beta\text{-Ga}_2\text{O}_3$ peaks, which shows a shift towards lower angles with higher In amounts

6. Effect of indium as a surfactant in $(\text{Ga}_{1-x}\text{In}_x)_2\text{O}_3$ epitaxial growth on Ga_2O_3

After having identified the solubility limit of In in Ga_2O_3 , we studied the effect of introducing small amounts of In during the growth of homoepitaxial Ga_2O_3 layers. $(\text{Ga}_{1-x}\text{In}_x)_2\text{O}_3$ layers were grown on (100) Ga_2O_3 substrates, providing an Ar flow through TMIIn-bubbler that was varied between 0 and 200 sccm. In order not to grow an In-rich $(\text{Ga}_{1-x}\text{In}_x)_2\text{O}_3$ alloy but to limit the In incorporation below 3%, the reactor pressure has been set at 50 mbar. The results obtained with these growth parameters can be classified in two main groups, depending on different TMIIn amount injected in the reactor.

The samples grown with Ar/TMIIn in the range 75-200 sccm present a particular surface morphology, as shown in Figure 12(a). The layers exhibit the presence of 1-5 μm wide and 1-2 nm high terraces, with an elongated and quite irregular shape, whose long axis is perpendicular to the [001] step down direction of the substrate. On the surface of the terraces it can be observed that the growth of the layers took place with a step-flow mechanism, shown in the AFM picture of Figure 12(b). The steps are ~ 600 pm high and 50-100 nm wide, mimicking the morphology of the Ga_2O_3 substrate surface prior to the growth. The morphological properties of the layers did not change significantly at different Ar/TMIIn flows, in the range 75-200 sccm.

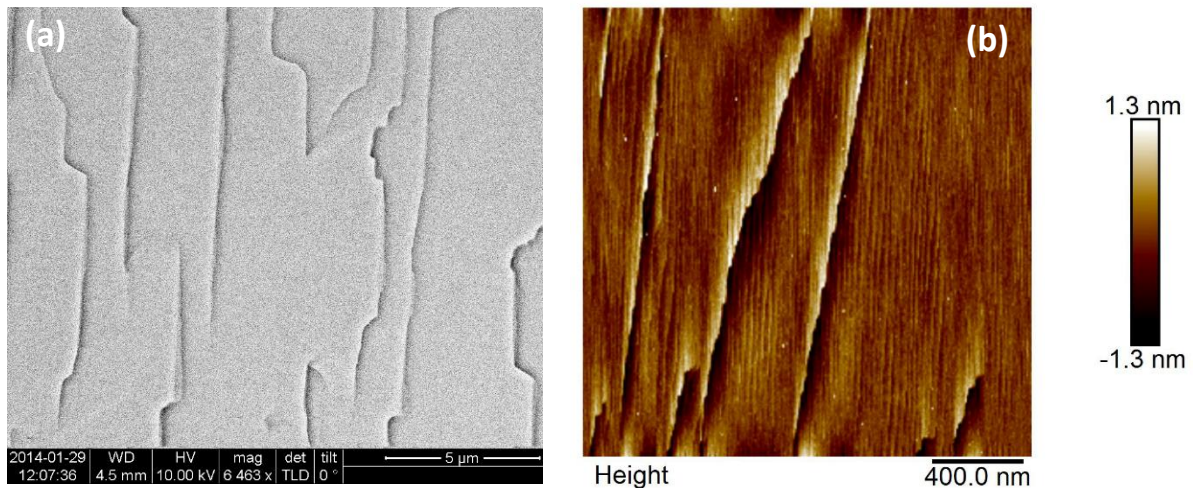


Fig. 12: Scanning electron microscopy (SEM) (a) and AFM (b) images of a $(\text{Ga}_{1-x}\text{In}_x)_2\text{O}_3$ layer grown on $\beta\text{-Ga}_2\text{O}_3$ with an Ar/TMIn flow in the range 75-200 sccm

On the contrary, if the Ar/TMIn flow is lower than 75 sccm, the morphology of the layers is completely different. Terraces and steps are not visible anymore, while a high amount of small defects appears, as shown in Figures 13. The number of these defects increases with the reactor pressure.

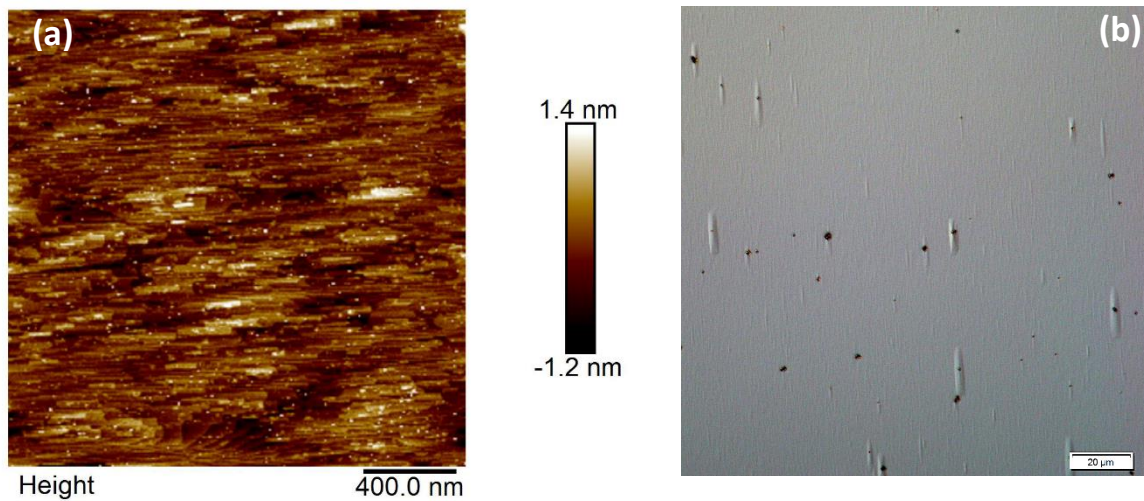


Fig. 13: AFM (a) and optical microscope (b) images of a $(\text{Ga}_{1-x}\text{In}_x)_2\text{O}_3$ layer grown on $\beta\text{-Ga}_2\text{O}_3$ with an Ar/TMIn flow < 75 sccm

$(\text{Ga}_{1-x}\text{In}_x)_2\text{O}_3$ epitaxial layers grown with different In flux TMIn were characterized by TEM and high resolution high-angle annular dark-field (HAADF) STEM. Fig.14(a) shows a typical cross sectional TEM micrograph of a (100)-oriented layer grown with Ar/TMIn flow in the effective 75-200 sccm range. The layer has a very high crystalline perfection. In contrast, layers grown with Ar/TMIn flow below 75 sccm have a very different crystal structure and exhibiting a high density of stacking faults and twins, see Figure 14(b).

This result has been explained, in analogy to the growth of GaN [15-17], by the tendency of In to float on the surface of Ga_2O_3 , delivering a surfactant effect that promotes a step-flow growth mode.

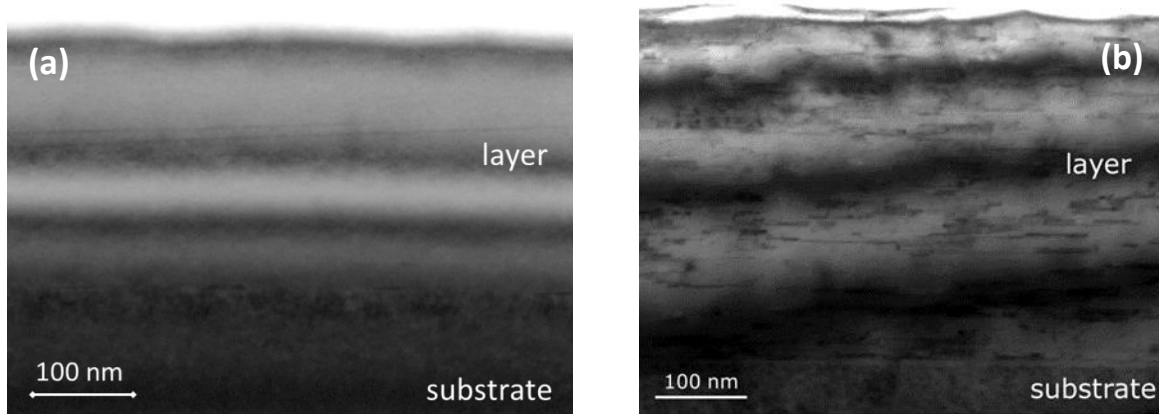


Fig. 14: TEM images of (a) $(\text{Ga}_{1-x}\text{In}_x)_2\text{O}_3$ and (b) Ga_2O_3 layers grown on $\beta\text{-Ga}_2\text{O}_3$. The concentration of stacking faults decreases dramatically thanks to the surfactant effect

7. n-type doping of $\beta\text{-Ga}_2\text{O}_3$ layers

7.1 Ga_2O_3 layers doped by Si using tetraethylorthosilicate ($\text{Si}(\text{OC}_2\text{H}_5)_4$)

Prerequisites for applying of Ga_2O_3 layers in power electronic and sensor devices are a high crystalline structure with low density of lattice defects and a net donor concentration in the range of 10^{17} up to 10^{19} cm^{-3} . For a long time the unintentional n-type conductivity of $\beta\text{-Ga}_2\text{O}_3$ has been attributed to an oxygen deficiency which leads to oxygen-vacancies (V_{O}) or Ga-interstitials (Ga_i). Recently, theoretical studies showed that (V_{O}) act as deep donors and do not contribute to the conductivity [18]. Therefore, doping with elements acting as shallow donors is necessary to enable growth of $\beta\text{-Ga}_2\text{O}_3$ with the electrical conductivity demanded by applications. Si and Sn atoms on the Ga site behave as a donor in $\beta\text{-Ga}_2\text{O}_3$. Si^{4+} ($r_{\text{ion}}=0.39 \text{ pm}$) can replace the Ga^{3+} ($r_{\text{ion}}=0.62 \text{ pm}$) site more easily than Sn^{4+} ($r_{\text{ion}}=0.69 \text{ pm}$) because of its smaller ion radius compared to Sn. Therefore, we have decided to explore the incorporation of Si in $\beta\text{-Ga}_2\text{O}_3$ layers grown by MOCVD method [19]. The optimized growth conditions for pure Ga_2O_3 films were applied also for the Si doping experiments. In a first time, we used Al_2O_3 (0001) wafers as substrates. Tetraethylorthosilicate ($\text{Si}(\text{OC}_2\text{H}_5)_4$ – TEOS) was chosen as a MO-source of Si. The molar flux of TEOS was changed from 10^{-7} to 10^{-9} mol/min .

All Si-doped $\beta\text{-Ga}_2\text{O}_3$ samples possess very smooth surface morphology as revealed by AFM. Roughness values in the range of 200 – 400 pm were measured. The Si incorporation in the lattice of selected samples was confirmed by secondary ion mass spectroscopy (SIMS) measurements. The distribution of Si through the sample thickness was homogenous. The concentration of Si (as chemical element) in the investigated layers varies between $4 \times 10^{17} \text{ cm}^{-3}$ and $5 \times 10^{19} \text{ cm}^{-3}$ as shown in Figure 15 for four $\beta\text{-Ga}_2\text{O}_3$ samples. Despite these high concentrations of Si, the samples do not show high conductivity. The resistivity decreased only slightly as a result of the doping. It is not yet clear whether this depends on incorporation of Si as electrically inactive species, for example in interstitial sites, or on self-compensation effects. To activate the Si donors some additional annealing procedures for 1 h and 30 min at a temperature ranging from 850 to 1050°C in O_2 and N_2 atmosphere were performed. Some layers were annealed in forming gas (5% H_2 in Ar) at temperatures of 600 and 700°C for 15 min. However, neither one type of annealing has changed the resistivity of the samples, i.e. they remained insulating.

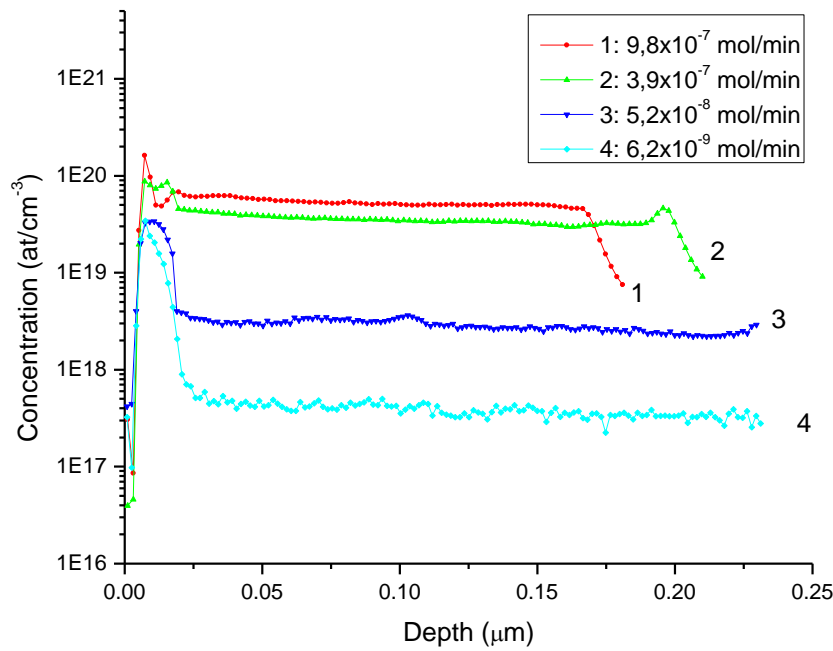


Fig. 15: SIMS depth profiles of four β -Ga₂O₃ samples with different Si concentration in the gas atmosphere

7.2 Ga₂O₃ layers doped by Sn using tetraethyltin (Sn(CH₃)₄)

Since the doping by Si donors was not effective to get semiconducting layers we have decided to use Sn, which is known as a successful donor in bulk crystal growth or in β -Ga₂O₃ layers. As a tin source we have taken tetraethyltin (TESn). The reactor base pressure in this series of experiments was changed from 5 to 20 mbar and the tin flux was adjusted between 3×10^{-11} and 1×10^{-8} mol/min. At a deposition temperature of about 800 °C layers with thickness between 90 and 550 nm, at a growth rate from 2 up to 5 nm/min, have been grown with Sn concentration in the range from 5×10^{19} to 1×10^{18} cm⁻³. Figure 16 shows the SIMS depth profile of three Ga₂O₃:Sn layers with a chemically incorporated Sn concentration between $1,3 \times 10^{18}$ and $2,3 \times 10^{18}$ cm⁻³. Increasing the Sn-flux in the growth atmosphere by one order of magnitude the chemical Sn-concentration in the layers increases of about 40 %. Figure 17 illustrates three typical XRD spectra of layers grown at equivalent conditions on Al₂O₃(0001) with different Sn doping. At a chemical Sn concentration of 1×10^{18} cm⁻³ the characteristic XRD pattern of β -Ga₂O₃ with the (-201), (-402), (-603) and (-804) Bragg reflections are visible, proving the epitaxial relationship between (-201) β -Ga₂O₃ planes and the (0001) Al₂O₃ ones. At higher Sn-doping (3×10^{18} cm⁻³) the (-201) and the (-603) Bragg peaks disappear (red curve). Further increase of doping might bring amorphization of the films (black curve).

Our experiments with MOVPE β -Ga₂O₃ doped with Si and Sn in the same range, as grown and exposed to annealing in O₂ or N₂, however, provided non-conductive material.

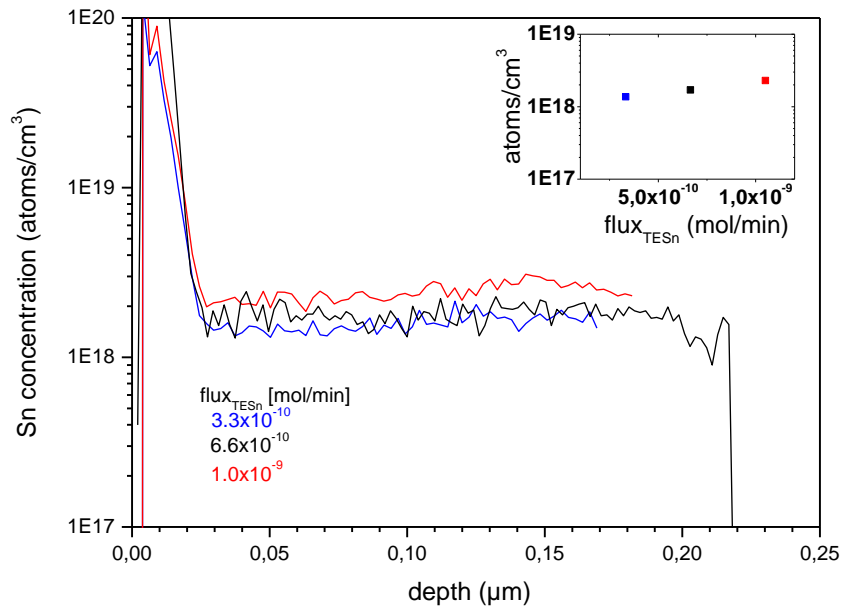


Fig. 16: SIMS depth profile of three β -Ga₂O₃ layers grown with different Sn-flux in the atmosphere. Inset graph shows the dependence of the Sn-concentration on the Sn-flux

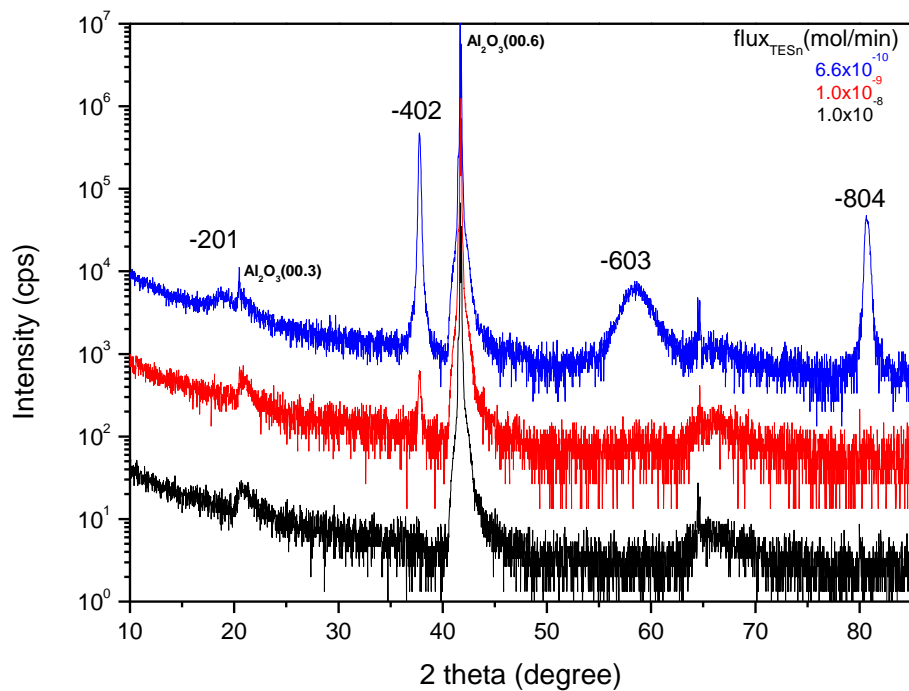


Fig. 17: XRD spectra of three layers grown at equivalent growth parameters but with different Sn-flux, given in the legend

8. β -Ga₂O₃ deposition by using triethylgallium (TEGa) and pure oxygen

In the first and second year of the project, we used TMGa and water as Ga and oxygen source and TESn as Sn-precursor [12, 13, 19]. Nevertheless, we were not able to achieve conductive layers. Independently from oxygen/TMGa ratio and additional thermal annealing steps the growth experiments did not provide reproducible conductive Ga₂O₃ layers. We assumed that the high carbon content in the growth atmosphere, deriving from the MO-precursors, contributes to the high resistivity in the layers. Theoretical studies [18, 20] have shown that also the formation of Ga vacancies at oxygen rich conditions may have even negative formation energy and can compensate the incorporated donors. From the MOVPE growth of GaAs [21] and GaN [22], it is known that the decomposition of TEGa-precursor in comparison to TMGa delivers much less free carbon and C₂H₅-groups, which do not effectively interact with the growth surface in comparison to TMGa and CH₃ groups. With respect to this knowledge, we have replaced TMGa by TEGa to reduce the carbon content in the grown layers. In addition, we performed the layer deposition at a reduced oxygen/TEGa-ratio of about 100 and to support the activation of the incorporated donor atoms we increased the deposition temperature to 850 °C. In comparison to TMGa based growth runs, by using TEGa and O₂ the temperature window to grow crystalline material resulted to be wider, starting at 650 °C instead of 750 °C. This effect could be attributed to the lower decomposition temperature of TEGa, due to its peculiar decomposition mechanism based on β -hydride elimination [23]. The optimal growth temperature was identified to be 850 °C, since at these conditions the surface of the layers presented the highest flatness and homogeneity. The AFM image in Figure 18 shows a typical surface morphology with a mean roughness of ~ 800 pm.

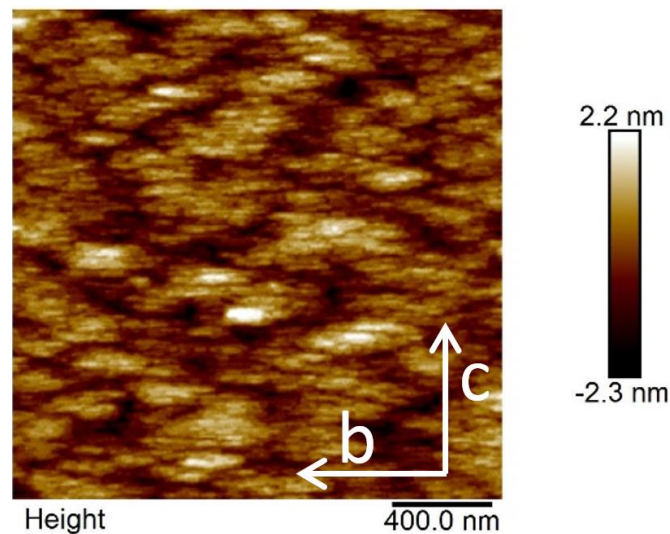


Fig. 18: AFM image of a β -Ga₂O₃ homoepitaxial layer grown with TEGa and O₂

Figure 19 shows the Sn-SIMS depth profiles of five Ga₂O₃ layers grown with a TESn flux between 4.6×10^{-12} and 6.6×10^{-10} mol/min, resulting in a chemical Sn incorporation from 2×10^{17} cm⁻³ up to 4×10^{19} cm⁻³, respectively. The layer thickness is about 160 nm. By increasing the TESn-flux in the growth atmosphere by two orders of magnitude the chemical Sn concentration in the layers increased nearly in the same range. In addition, the SIMS profiles demonstrate that at a TESn-flux of 4.6×10^{-12} mol/min the chemical Sn concentration in the layer is in the same range as in an unintentional doped layer. Therefore, we conclude that the background doping level in the layers is in the beginning of 10^{17} cm⁻³ as a result of Sn-pollution in the reactor and additional memory effects after long time deposition of Sn-doped layers.

All the Sn doped layers have shown n-type conductivity. By Hall-measurements, it was found that while the mobility fluctuates around 25 cm²/Vs, the carrier concentration increases from 5×10^{17} cm⁻³ to 3×10^{18} cm⁻³ by increasing the TESn-flux in the growth atmosphere. The highest

mobility ($41 \text{ cm}^2/\text{Vs}$) was observed at a carrier concentration of $1 \times 10^{18} \text{ cm}^{-3}$. Such mobility value, to the best of our knowledge, is the highest one obtained for $\beta\text{-Ga}_2\text{O}_3$ layers grown by MOVPE. Figure 20 shows the dependence of the net donor concentration (left y axis) and the chemical Sn concentration (right y axis) in dependence on the TESn-flux in the gas atmosphere. It can be observed that at TESn-fluxes lower than $5 \times 10^{-11} \text{ mol/min}$ the chemical Sn concentration is below the estimated net carrier concentration. This may indicate the existence of other doping elements or point defects that can influence the electrical properties. SIMS measurements relative to carbon in the Sn-doped layers delivered chemical concentration in the beginning of 10^{17} cm^{-3} . These results are not completely reliable because it is very difficult to distinguish between the carbon background of the SIMS-system and the real C-concentration in the layers. A more detailed investigation is necessary to understand the role of carbon and its interaction with structural defects and its influence on the electrical properties of the layers.

Summarizing, we have shown that Sn is an effective n-type dopant for Ga_2O_3 and that the free carrier concentration can be controlled over one order of magnitude by varying the TESn-flux in the gas phase during layer deposition.

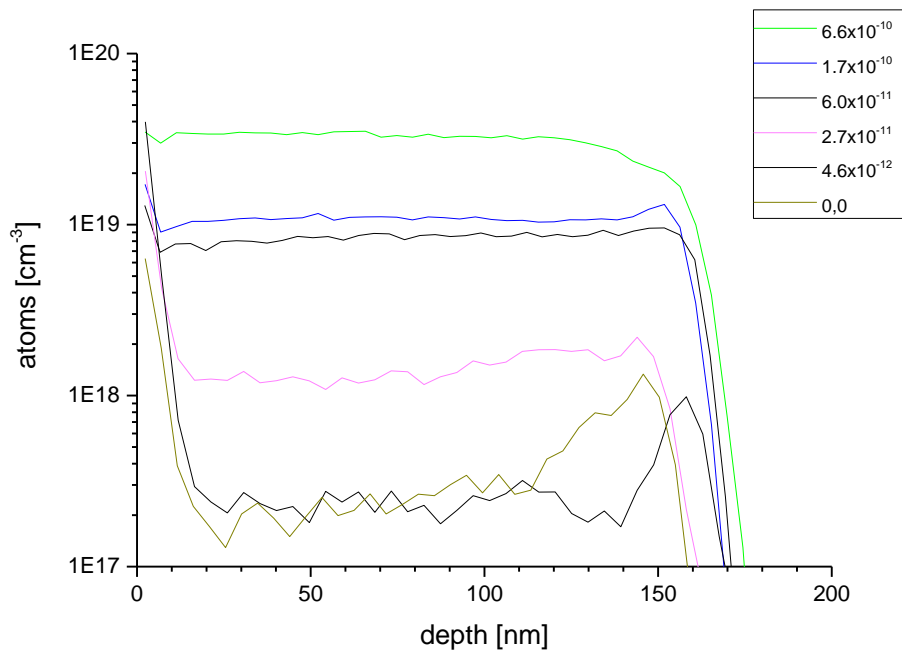


Fig. 19: SIMS Sn depth profiles of $\beta\text{-Ga}_2\text{O}_3$ layers grown at 850°C with different TESn-flux, expressed in mol/min

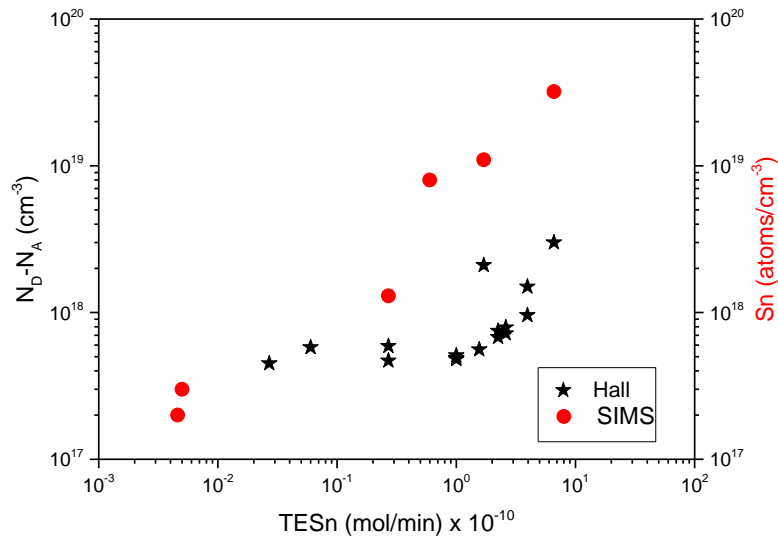


Fig. 20: Net carrier concentration, $N_D - N_A$, (Hall) and chemical Sn concentration (SIMS) in dependence on the TESn-flux in the growth atmosphere

9. Summary

β -Ga₂O₃ epitaxial layers were successfully grown on α -Al₂O₃ (0001) and β -Ga₂O₃ (100) substrates using metal-organic vapour phase epitaxy. Trimethylgallium or triethylgallium and pure oxygen or water were used as precursors for gallium and oxygen. With pure oxygen, it was not possible to deposit smooth and coherent homoepitaxial layers independently of the growth parameters. When using water as oxidant, we succeeded to grow smooth homoepitaxial β -Ga₂O₃ layers. The presence of hydrogen had a positive effect on kinetic conditions of the substrate surface and hence supported the layer-by-layer growth. The layers grown on sapphire had an epitaxial relationship (-201) β -Ga₂O₃ || (0001) Al₂O₃. On β -Ga₂O₃ (100) substrates the layers were single crystalline with (100)-orientation. Stacking faults and twins were the main defects that influenced the crystalline perfection of the materials.

By using a sufficiently high amount of In precursor, indium showed an essential role in limiting the concentration of crystallographic defects, promoting the step-flow growth of the layers. High quality epitaxial layers of the mixed (Ga_{1-x}In_x)₂O₃ phase were grown with trimethylgallium and H₂O as precursors. No In₂O₃ separated phase was observed up to $x \sim 0.25$. Layers grown with Ar/TMIn flow in the effective 75-200 sccm range have a very high crystalline perfection. In contrast, layers grown with Ar/TMIn flow below 75 sccm have a very different crystalline perfection and a high density of stacking faults and twins.

When TMGa and water were used as Ga and oxygen source and tetraethyltin (TESn) or tetraethylorthosilicate (TEOS) as Sn or Si precursor, no conductive layers were achieved. Independently from oxygen/TMGa ratio and additional thermal annealing steps after layer deposition no increase of the conductivity in the layers was measured. In order to decrease the C incorporation in the layers, which could be one of the origins of the high resistivity, TMGa was replaced by TEGa. By additionally reducing the oxygen/TEGa ratio and increasing the deposition temperature to 850 °C, all the Sn-doped layers resulted to be conductive. Sn was incorporated from 10¹⁸ cm⁻³ up to beginning of 10²⁰ cm⁻³ by tuning the TESn flux. By electrical measurements, it was observed that while the mobility fluctuated around 25 cm²/Vs, the carrier concentration increased from 5 × 10¹⁷ to 5 × 10¹⁸ cm⁻³ by increasing the TESn-flux in the growth atmosphere. The highest mobility value of 41 cm²/Vs, which represents a record for β -Ga₂O₃ layers grown by MOVPE, was observed at a carrier concentration of 1 × 10¹⁸ cm⁻³.

10. Technical applicability of the scientific results

To evaluate their structural and electronic quality for application in deep UV-detectors and medium/high voltage electronic devices (FETs), homoepitaxial n-type β -Ga₂O₃ layers have been delivered to academic partners of the Institute for Crystal Growth.

A set of samples was sent to the Leipzig University, Institute for Experimental Physics, in order to realize deep-UV-sensitive detectors. This activity has been started in March 2015.

To verify the application potential in metal-semiconductor field-effect transistors, a set of sample went to Ferdinand-Braun-Institute, Berlin. This activity started in February 2015.

Both new application oriented projects are currently underway and the first results will be expect in the second half of 2015. The aim of these activities is the production of working demonstrator devices. On this basis a new project will be prepared directly in cooperation with an industrial partner or in frame of an application-oriented research program.

After the end of the project a joint research project with the Department of Physics, Humboldt-University, Berlin, has been created. The proposal was submitted to the DFG in July 2015.

11. Educate and qualification activities

In the project work, a PhD student was involved as a young scientist. In his thesis, the PhD student will investigate the atomic structures of binary and ternary metal oxide thin films through transmission electron microscopy. In the focus of this investigation will be the generation of structural and point defect and their correlation to the electrically properties of the films.

The PhD work has been started in summer 2012 and is currently in its final stage. The official conclusion has been fixed for end of 2015.

12. Dissemination and storing of the scientific results

All scientific results in relation to the successful fulfilled project were published in peer-reviewed journals, presented at international conferences, workshops or meetings. The publication of at least one article about the last results is currently in preparation.

The PhD-thesis will be defended at the Humboldt-University, department of Physics, in 2016.

The logbook and all laboratory documents are stored as digital files in the institute.

All the epitaxial layers produced in the frame of the project are available in our institute for further scientific cooperation or for future joint projects.

Literature:

- [1] R. Suzuki, S. Nakagomi, Y. Kokubun, N. Arai, S. Ohira, Appl. Phys. Lett. **94**, 222102 (2009)
- [2] D. Guo, Z. Wu, P. Li, Y. An, H. Liu, X. Guo, H. Yan, G. Wang, C. Sun, L. Li, and W. Tang, Opt. Mater. Express **4**, 1067-1076 (2014)
- [3] M. Higashiwaki, K. Sasaki, A. Kuramata, T. Masui, S. Yamakoshi, Phys. Status Solidi A **211**, 21 (2014)
- [4] M. Higashiwaki, K. Sasaki, A. Kuramata, T. Masui, S. Yamakoshi, Appl. Phys. Lett. **100**, 013504 (2012)
- [5] K. Sasaki, M. Higashiwaki, A. Kuramata, T. Masui, S. Yamakoshi, J. Cryst. Growth **378**, 591 (2013)
- [6] S. Ohira, N. Arai, T. Oshima, S. Fujita, Appl. Surf. Science **254**, 7838 (2008)
- [7] Z. Gałazka, R. Uecker, K. Irmischer, M. Albrecht, D. Klimm, M. Pietsch, M. Bruetzam, R. Bertram, S. Ganschow, R. Fornari, Cryst. Res. Technol. **45**, 1229 (2010)
- [8] Z. Gałazka, K. Irmischer, R. Uecker, R. Bertram, M. Pietsch, A. Kwasniewski, M. Naumann, T. Schulz, R. Schewski, D. Klimm, M. Bickermann, Journal of Crystal Growth **404**, 184 (2014)
- [9] Z. Gałazka, R. Uecker, K. Irmischer, D. Schulz, D. Klimm, M. Albrecht, M. Pietsch, S. Ganschow, A. Kwasniewski, R. Fornari, J. Crystal Growth **362**, 349 (2013)
- [10] Z. Gałazka, R. Uecker, D. Klimm, K. Irmischer, M. Pietsch, R. Schewski, M. Albrecht, A. Kwasniewski, S. Ganschow, D. Schulz, C. Guguschev, R. Bertram, M. Bickermann, R. Fornari, Phys. Status Solidi A **211**, 66 (2014)
- [11] Z. Gałazka, D. Klimm, K. Irmischer, R. Uecker, M. Pietsch, R. Bertram, M. Naumann, A. Kwasniewski, R. Schewski, M. Bickermann; Phys. Status Solidi A (2015), DOI 10.1002/pssa.201431835
- [12] G. Wagner, M. Baldini, D. Gogova, M. Schmidbauer, R. Schewski, M. Albrecht, Z. Gałazka, D. Klimm, R. Fornari; Phys. Status Solidi (a) **211**, 27 (2014)
- [13] M. Baldini, D. Gogova, K. Irmischer, M. Schmidbauer, G. Wagner, R. Fornari; Cryst. Res. Technol. **49**, 552 (2014)
- [14] F. Zhang, K. Saito, T. Tanaka, M. Nishino, Q. Guo; Solid State Comm. **186**, 28 (2014)
- [15] S. Keller, S. Heikman, I. Ben-Yaacov, L. Shen, S. P. DenBaars and U. K. Mishra, Appl. Phys. Lett. **79**, 3449 (2001)
- [16] J. E. Northrup and C. G. Van de Walle, Appl. Phys. Lett. **84**, 4322 (2004)
- [17] D. Won, X. Weng and J. M. Redwing, Appl. Phys. Lett. **100**, 021913 (2012)
- [18] J. B. Varley, J. R. Weber, A. Janotti, C.G. Van de Walle; Appl. Phys. Lett. **97**, 142106 (2010)
- [19] D. Gogova, G. Wagner, M. Baldini, M. Schmidbauer, K. Irmischer, R. Schewski, Z. Gałazka, M. Albrecht, R. Fornari, J. Cryst. Growth **401**, 665 (2014)
- [20] J. B. Varley, H. Peelaers, A. Janotti, C. G. van de Walle, J. Phys: Condens. Matter **23**, 334212 (2011)
- [21] A.A. Aquino, T.S. Jones, Appl. Surf. Sci. **104/105**, 304 (1996)

- [22] A. Saxler, D. Walker, P. Kung, X. Zhang, M. Razeghi, J. Solomon, W. C. Mitchel, H. R. Vydyanath, Appl. Phys. Lett. **71**, 3272 (1997)
- [23] M. Yoshida, H. Watanabe, F. Uesugi, J. Electrochem. Soc. **132**, 677 (1985)

Publications

- G. Wagner, M. Baldini, D. Gogova, M. Schmidbauer, R. Schewski, M. Albrecht, Z. Galazka, D. Klimm, R. Fornari; **Homoepitaxial growth of β -Ga₂O₃ layers by metal-organic vapor phase epitaxy**; Phys. Status Solidi A 211 (2014) 27 – 33
- D. Gogova, G. Wagner, M. Baldini, M. Schmidbauer, K. Irmscher, R. Schewski, Z. Galazka, M. Albrecht, R. Fornari; **Structural Properties of Si-doped β -Ga₂O₃ layers grown by MOVPE**; J. Cryst. Growth 401 (2014) 665 – 669
- M. Baldini, D. Gogova, K. Irmscher, M. Schmidbauer, G. Wagner, R. Fornari; **Heteroepitaxy of Ga_{2(1-x)In_{2x}O₃ layers by MOVPE with two different oxygen sources}**; Cryst. Res. Technol. 49, No. 8 (2014) 552 – 557
- M Baldini, M Albrecht, D Gogova, R Schewski, G Wagner; **“Effect of indium as a surfactant in (Ga_{1-x}In_x)₂O₃ epitaxial growth on β -Ga₂O₃ by metal organic vapour phase epitaxy”**, Semiconductor Science Technology, Semicond. Sci. Technol. 30 (2015) 024013
- R. Schewski, G. Wagner, M. Baldini, D. Gogova, Z. Galazka, R. Uecker, T. Schulz, T. Remmele, T. Markurt, H. von Wenckstern, M. Grundmann, O. Bierwagen, Patrick Vogt, M. Albrecht; **“Strain induced Stabilization of α -Ga₂O₃ in the epitaxial growth of Ga₂O₃ on Al₂O₃ (0001)”**; Applied Physics Express 8 (2015) 011101
- E. Korhonen, F. Tuomisto, D. Gogova, G. Wagner, M. Baldini, Z. Galazka, R. Schewski, M. Albrecht; **“Electrical compensation by Ga vacancies in Ga₂O₃ thin films”**; Applied Physics Letters 106 (2015) 242103

Oral contributions to conferences

- G. Wagner, M. Baldini, D. Gogova, M. Schmidbauer, R. Schewski, M. Albrecht, D. Klimm; **Homoepitaxial growth of β -Ga₂O₃ by metal-organic vapor-phase epitaxy**; 2013 MRS Fall Meeting & Exhibit (Boston, USA, 2013, 02.-05.12.)
- G. Wagner, M. Baldini, D. Gogova, M. Schmidbauer, R. Schewski, M. Albrecht; **Ga₂O₃ and (Ga_{1-x}In_x)₂O₃ layers on beta-Ga₂O₃(100) grown by metal organic vapor phase epitaxy**; TCO2014 (Leipzig, Germany, 2014, 29.09-02.10)
- G. Wagner, M. Baldini, D. Gogova, M. Albrecht, K. Irmscher; **Homo- and heteroepitaxial growth of beta-Ga₂O₃ layers by MO-VPE**; E-MRS Fall-meeting (Warszawa, Poland, 2014, 15.-18.11.)
- G. Wagner, M. Baldini, D. Gogova, M. Schmidbauer, M. Albrecht, D. Klimm, R. Schewski; **Influence of the different oxygen precursors on layer growth and the properties of Ga₂O₃ layers by using MOVPE**; 14. Kinetik Seminar der DGKK, (Berlin, Germany, 2013, 21.-22.11.)
- D. Gogova, G. Wagner, M. Baldini, K. Irmscher, M. Albrecht, R. Schewski, M. Schmidbauer, A. Kwasniewski, Z. Galazka; **Gallium Oxide – A Newly Rediscovered Wide Bandgap Semiconductor**, Collaborative Conference on Crystal Growth, Recent Advances in Growth of Wide Bandgap Materials Workshop (Phuket, Thailand, 2014, 3.-5.11)

M. Baldini, G. Wagner, D. Gogova; **Ga₂O₃ layers grown by metal organic vapor phase epitaxy with two different Ga and O precursors**, MRS Spring Meeting (San Francisco, USA, 2015, 6.-10.04)

Posters

M. Baldini, M. Albrecht, D. Gogova, K. Irmscher, R. Schewski, M. Schmidbauer, G. Wagner; **(Ga_{1-x}In_x)₂O₃ layers grown by metal organic vapour phase epitaxy**, CIMTEC 2014, 6th Forum on New Materials (Montecatini Terme, Italy, 2014, 15.-19.06)

M. Baldini, M. Albrecht, D. Gogova, K. Irmscher, R. Schewski, M. Schmidbauer, G. Wagner, **Heteroepitaxy of (Ga_{1-x}In_x)₂O₃ layers by MOVPE with different oxygen sources**, ICG 2013, Italian Crystal Growth Conference (Parma, Italy, 2013, 14.-15.11)

C.E. Tommaseo, G. Wagner, M. Baldini; **XAFS analyses of homo- and heteroepitaxial grown β-Ga₂O₃ films on β-Ga₂O₃ and Al₂O₃ substrates**, BESSY User Meeting (Berlin, Germany, 2014, 02.12.)

E. Korhonen, F. Tuomisto, D. Gogova, G. Wagner, M. Baldini and Z. Galazka, **Vacancy defects in homo- and heteroepitaxial Ga₂O₃ thin films**, Int. Workshop Positron Studies Defects (PSD-14) (Kyoto, Japan, 2014, 14-19.09)

Scientific staff that was involved in the project work:

MOCVD-team:

Dr. Günter Wagner
Dr. Michele Baldini
Dr. Daniela Gogova
Raimund Grüneberg, technician

X-ray characterization:

Dr. Martin Schmidbauer
Dipl. Phys. Albert Kwasniewski

Physical characterization:

Dr. Klaus Irmscher
Mike Pietsch, technician

TEM-characterization:

Dipl. Phys. Robert Schewski, PhD student
Dr. Martin Albrecht

Thermodynamic calculations:

Dr. Detlef Klimm

Growth of the bulk material:

Dr. Zbigniew Galazka